

Theory of light propagation in strongly modulated photonic crystals: Refractionlike behavior in the vicinity of the photonic band gap

M. Notomi*

NTT Basic Research Laboratories, 3-1 Morinosato-Wakamiya, Atsugi, Kanagawa 243-0198, Japan

(Received 7 April 2000)

Although light propagation in weakly modulated photonic crystals is basically similar to propagation in a diffraction grating in which conventional refractive index loses its meaning, we demonstrate that light propagation in strongly modulated two-dimensional (2D)/3D photonic crystals becomes refractionlike in the vicinity of the photonic bandgap. Such a crystal behaves as a material having an effective refractive index controllable by the band structure. This situation is analogous to the effective-mass approximation in electron-band theory. By utilizing this phenomenon, negatively refractive material can be realized, which has interesting optical properties such as mirror-image refraction.

I. INTRODUCTION

A photonic crystal is a structure whose refractive index is periodically modulated, and the resultant photonic dispersion exhibits a band nature analogous to the electronic band structure in a solid. The one-dimensional (1D) version of a photonic crystal has long been known as a multilayer reflector, but 2D/3D photonic crystals have only recently started to attract attention after the appearance of a prediction that photonic insulators can be developed by photonic crystals.¹ Since then, photonic crystals have become a major subject of today's photonic engineering research.² So far, most of the concern has been focused on their potential as photonic insulators.³ However, they can also be photonic conductors whose conductance is determined by their band structure.⁴ In photonic crystals, light travels as Bloch waves, in a similar way to plane waves in continuous material. Bloch waves travel through crystals with a definite propagation direction despite the presence of scattering, but their propagation is complicated because it is influenced by the band structure.

In this paper, we investigate the situation shown in Fig. 1. A light beam is traveling through different media. If the medium is a dielectric material, then we observe conventional refraction phenomenon. If the medium is a diffraction grating, then we observe diffraction phenomenon. Then, what kind of light propagation phenomena would be observed if the medium is a photonic crystal? There have been some works related to this issue in the literature, but systematic and consistent way of understanding is still lacking. Therefore, we will now start from the simple cases of a dielectric material and a diffraction grating and then examine photonic crystals with weak and strong periodic modulation effects, in order to obtain a systematic view for propagation in periodic structures and, in particular, photonic crystals. We will clarify features of light propagation in photonic crystals, and show how a strongly modulated photonic crystal exhibits remarkably interesting propagation characteristics which can be understood as refractionlike phenomenon in standard geometrical optics with unusual refractive index.

II. ANOMALOUS LIGHT PROPAGATION IN PHOTONIC CRYSTALS?

Unusual light propagation in photonic crystals has been remarked upon by several authors.⁵⁻⁹ Lin *et al.* reported that refraction angle becomes anomalous near the bandgap.⁶ Kosaka *et al.* reported that, under certain conditions, the light propagation direction in photonic crystals becomes very sensitive to the incident angle and wavelength, and large beam steering is observed, which they call superprism phenomenon.⁷ However, almost the same phenomena were observed in 1D and 2D grating wave guides,⁵ and the distinction between behavior in photonic crystals and that in grating wave guides is not clear. In addition to that, there have been some theoretical reports that predict unusual refractive index for photonic crystals.^{8,9}

The essential explanation of these phenomena should lie in the photonic band structure because the direction of light propagation inside the photonic crystal is determined by the equifrequency surface of the photonic bands in these structures.¹⁰ Although this feature of photonic crystals has been frequently discussed, there have been very few reports about quantitative comparison between theory and experiment so far.¹¹ Considering this feature, it might be possible to reconstruct the photonic band structure from measurements of the light propagation inside the photonic crystal. We recently demonstrated such an experiment for 3D Si/SiO₂ photonic crystals that were fabricated by auto-cloning technology,¹² and a very detailed photonic band structure was successfully obtained by the measurement.¹³ This experiment directly shows that the light propagation is

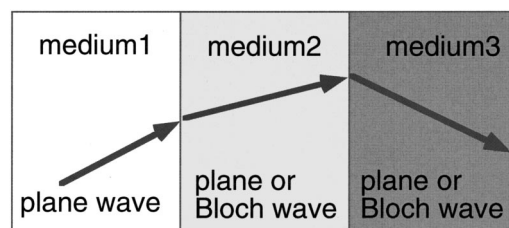


FIG. 1. Schematic diagram of light propagation phenomenon through different media.

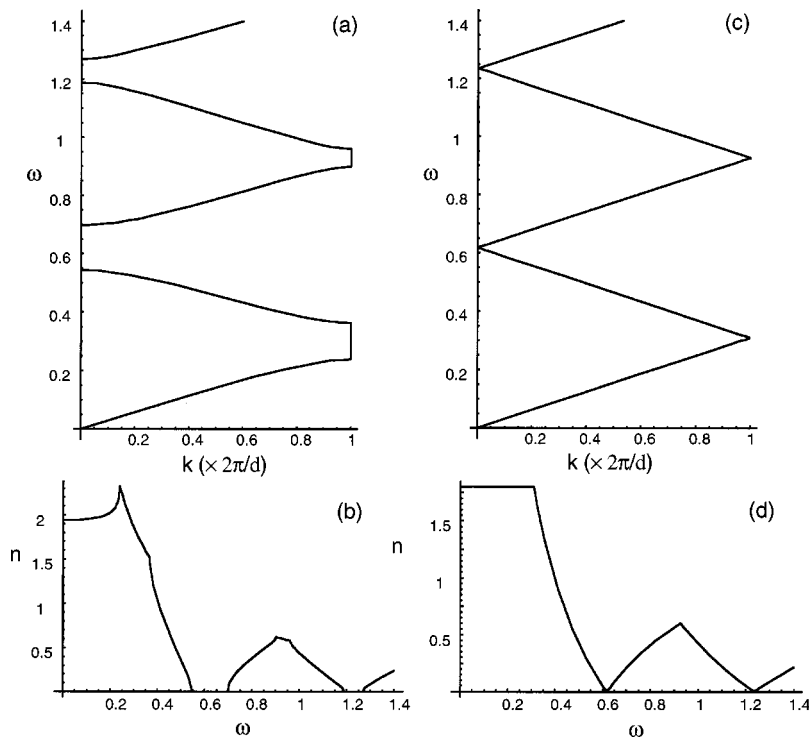


FIG. 2. (a) Photonic band diagram of a Si ($n=3.5$)/SiO₂ ($n=1.46$) multilayer (1D photonic crystal) structure with a period of d . The thickness is $0.15d$ and $0.85d$, respectively. (b) Deduced phase refractive index versus frequency for the multilayer structure. (c) Photonic band diagram of a 1D photonic crystal with a vanishingly small index modulation (empty lattice). The average index is the same as (a). (d) Deduced phase refractive index versus frequency for the empty lattice. Frequency is normalized as $\omega d/2\pi c$.

indeed determined by the photonic band structure. This means that, if we want to investigate the light propagation in photonic crystals, what we have to do is just to calculate the corresponding photonic band structure. However, photonic band structures are fairly complicated and it is thus not easy to understand the light propagation phenomena in photonic crystals in qualitative terms. Moreover, the relation between the light propagation in photonic crystals and that in conventional dielectric materials or gratings has yet to be clearly demonstrated. We believe that a simpler way of understanding light propagation in photonic crystals is possible and should be established, which will clarify the difference between behavior in photonic crystals and conventional refraction or diffraction phenomena.

As mentioned above, light propagation in photonic crystals is represented by Bloch waves. Bloch waves have a definite propagation direction in spite of strong scattering by the periodic structure. This character leads us to consider a geometrical optic approach to understand the propagation in it. In conventional geometrical optics in dielectric materials, light propagation—as shown in Fig. 1—is described by the phase refractive index and Snell's law. Therefore, in order to pursue geometrical approaches for photonic crystals, we will examine the concept of phase refractive index for photonic crystals.

The phase refractive index of photonic crystals has been discussed by several authors in the long wavelength limit.^{14–16} They have homogenized the periodic structures and deduced an appropriate phase index in the low-frequency limit. However, such a result cannot be extended to higher frequencies of which wavelength becomes comparable to, or smaller than, the lattice period. Since most of interesting phenomena, including unusual beam propagation, occur outside the low-frequency limit, we are not satisfied with this homogenization method to understand the light propagation in photonic crystals.

Lin *et al.* investigated the lowest band of a 2D photonic crystal near its first gap, and argued that the refractive index is modified from the low-frequency limit value near the gap because the slope of the dispersion curve is reduced.⁶ This effect is not significantly large because the control range of index is limited within refractive indices of materials. The present photonic crystal effect simply arises as a modification of the mixing ratio of index values, similar to the way in which the effective refractive index of a conventional slab wave guide is derived.¹⁷ Furthermore, their argument did not show whether the index they deduced could be meaningful outside the low-frequency limit (we will show later that such index is generally meaningless except under a certain condition), and it is not clear how this index is related to propagation direction.

To investigate the phase index of periodic structures outside the low-frequency limit, we must first consider the band-folding effect. To see this, we plot a photonic band diagram of a multilayer (1D photonic crystal) structure as in Fig. 2(a). If we simply use the textbook formula $n = ck/\omega$ for the phase refractive index, we obtain the result shown in Fig. 2(b). The resultant phase index exhibits very unusual behavior as can be seen in the figure. Dowling *et al.* used essentially the same argument to predict an ultrasmall index for photonic crystals.⁸ This effect is due to the reduction of wave vector k near the zone center as a result of the band folding. However, this argument leads to an ultrasmall n even for an empty lattice with the same crystal structure. Figure 2(c) is a band diagram of a 1D photonic crystal with an infinitely small index modulation. The corresponding phase index is shown in Fig. 2(d). We know that light propagation in such an empty-lattice photonic crystal (at least when its frequency does not satisfy the Bragg condition) should be normal; however, this model still predicts abnormal phase index. This apparent contradiction shows that the deduced small n does not possess real meaning and that the band folding itself does

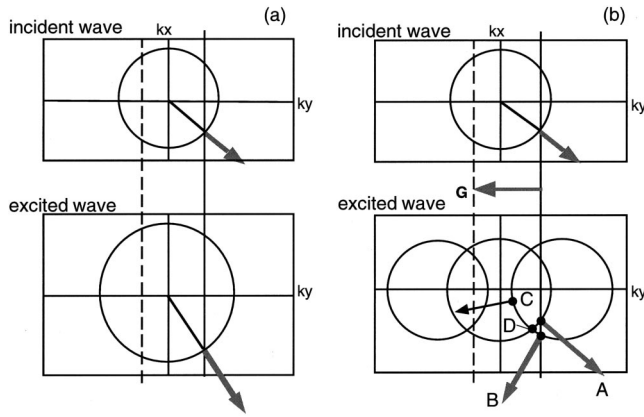


FIG. 3. (a) EFS plot for light incident problem from air to a dielectric material. (b) EFS plot for a diffraction grating.

not lead to unusual beam propagation. This contradiction arises mainly because we have only considered k in the above analysis. We must also consider the group velocity vector to study beam propagation in photonic crystals. We thus need to investigate the equifrequency surface (EFS) of the photonic band structure.

III. LIGHT PROPAGATION IN DIELECTRIC MATERIALS AND DIFFRACTION GRATINGS

In this section, we reexamine light propagation in dielectric materials and diffraction gratings by using EFS plots. Firstly, we show a very simple example of EFS analysis in Fig. 3(a), which describes a light incident problem from air to a dielectric material. A circle in the figure is an EFS of the photonic band of a dielectric, namely, $\omega = ck/n$. The k vector in the dielectric medium is determined by the continuity of tangential components of the k vector across the interface, and light always propagates parallel to the k vector in this case. This is an EFS expression of conventional refraction phenomenon, and this plot is a graphical representation of Snell's law in k space

$$n_1 \sin \theta_1 = n_2 \sin \theta_2. \quad (1)$$

In Fig. 3(b), we depict light propagation in a diffraction grating with a period of d . In this case, equifrequency circles are repeated along the periodic axis due to the grating's periodicity, and the k -conservation rule has to be generalized to satisfy the periodic boundary condition. As a result of this, applying the k conservation rule, we see that more than one nonidentical beams can be excited in a grating. In the figure, wave A (on a circle centered at the origin) corresponds to a transmitted wave and wave B (on a circle centered at a reciprocal lattice point) is a diffracted wave. This is nothing but beam decomposition by a diffraction grating. Note that the light propagation direction is not parallel to the k vector for a diffracted wave, but it is oriented normal to the diffracted wave circle. This is a graphical representation of the formula for a diffraction grating

$$m\lambda = d(\sin \theta_1 + \sin \theta_2). \quad (2)$$

Other than beam decomposition, a few points can be drawn from this figure. At point C (this point can be excited

under certain conditions), k is very close to the origin, which leads to very small phase index. However, this phase index cannot be used to express the light propagation direction because the propagation direction (indicated by the arrow) is not parallel to the k vector. In other words, this index is almost meaningless in terms of the light propagation problem. This directly demonstrates why the previous models including Dowling's^{8,9} are insufficient to describe the refraction phenomena. To analyze propagation phenomena, we have to examine the curvature of EFS.

Next, look at point D, which is an intersecting point of two circles. This point is a kind of singular points in k space. At such a point, the propagating direction becomes undefined, and generally anticrossing occurs between intersecting circles. Therefore, the propagation direction switches from one circle to the other in the vicinity of this point. That is, when we vary the incident angle or wavelength in the vicinity of this point, the beam propagation direction changes very rapidly. If we carefully choose the wavelength and incident angle to excite the vicinity of this intersecting point, the beam propagation direction becomes very sensitive to the incident angle and wavelength. This is the origin of the large beam steering observed in the grating wave guide. This is a general phenomenon, which occurs at singular points in k space, thus we call it singular point diffraction. Conical refraction¹⁷ in anisotropic media apparently has the same origin as singular point diffraction. The similar conical singularity has also been discussed in the electron band theory in the case of weak periodic modulation.¹⁸ In addition to that, to be precise, a gap opens up at such singular points, and we will discuss its influence in the next section.

From these discussions, it is now clear that we cannot define a phase index for a grating in terms of Snell's law. If we define a phase index, the index is strongly dependent on the incident angle or k -vector angle. Therefore, Snell's law loses its meaning. This means that the discussed phenomena in a grating cannot be understood within a refraction picture, and must be understood as diffraction.

IV. LIGHT PROPAGATION IN WEAKLY MODULATED PHOTONIC CRYSTALS

We now move on to the case for photonic crystals. First, we examine a 2D photonic crystal with a weak periodic modulation effect. Hereafter, we use a plane-wave expansion method,¹⁹ to calculate a photonic band diagram and EFS, in which Bloch waves are expanded by approximately 1000 plane waves. Frequency is normalized as $\omega a/2\pi c$ (a is the lattice constant). We examine mainly TE modes (magnetic field lies perpendicular to the 2D plane) of the structure, but the result obtained in this paper is not specific to TE modes.

The EFS of a hexagonal 2D photonic crystal with a vanishingly small index modulation is plotted in Fig. 4(a). The EFS in the first Brillouin zone is expanded to the outer reciprocal space. The EFS consists of repeated circles reflecting the 2D hexagonal periodicity, by the same mechanism as that in a 1D diffraction grating. If a plane wave is launched to this photonic crystal from air at a certain incident angle, several phenomena are expected from this figure. First, a light beam is decomposed into more than one nonidentical waves. In the situation in Fig. 4(a), two waves A and B are

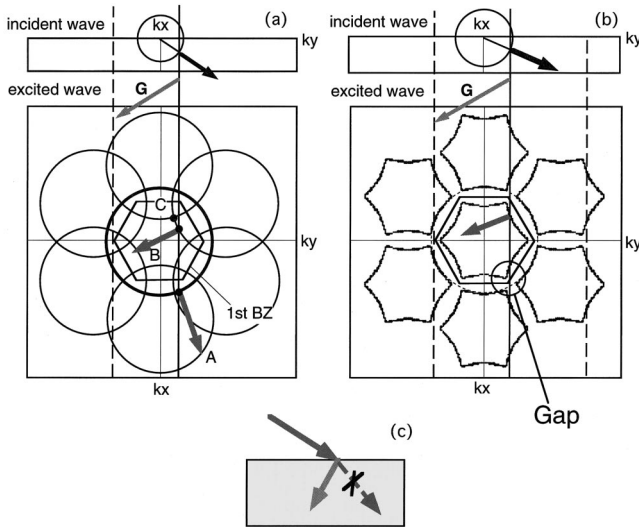


FIG. 4. (a) Schematic EFS plot for a hexagonal 2D photonic crystal with a vanishingly small index modulation. The first Brillouin zone (BZ) is shown as a hexagon. (b) EFS plot for a hexagonal 2D photonic crystal with finite index modulation. This EFS is calculated for TE mode in a 2D hexagonal GaAs ($n=3.6$) air-hole photonic crystal at $\omega=0.35$ which is far from the gaps, but this type of EFS is general for photonic crystals at frequencies far from the gaps or photonic crystals with a small index modulation. (c) Schematic of anomalous diffraction near the singular point.

excited. Wave A corresponds to a transmitted wave, and wave B is a diffracted wave. Second, the propagation direction is apparently not parallel to the k vector for diffracted waves. The propagation direction is oriented to the group velocity vector $\mathbf{v}_g = \text{grad}_k \omega$ which is normal to the EFS. Third, the propagation angle is very sensitive to the incident angle and wavelength if the launched beam excites the waves near intersecting points (e.g., point C), which leads to large beam steering. This is the origin of the superprism effect as reported in Ref. 7. Fourth, in some regions of the EFS near the Γ point, k vector becomes very small and it leads to a very small index value. But such an index is not meaningful by the same reason as for a grating. As readers already may have noticed, the situation as a whole is similar to that for a grating. The anomalous beam propagation in photonic crystals can be explained by the mechanism outlined above for a diffraction grating. Consequently, we still cannot define a proper phase refractive index for a weakly modulated photonic crystal which precisely reflects the light propagation.

In the above discussion, we investigated the effect of band folding for light propagation, which is mostly sufficient to understand gratinglike diffraction phenomena. If, however, the periodic modulation increases, another effect needs to be taken into account; the gap appears in EFS at the intersecting points. This is the seed for the photonic band gap. If we further enlarge the periodic modulation, this gap eventually comes to dominate the whole of k space and photonic band gaps will emerge. For now, however, we still stay with relatively small index modulation, which is actually the case for most of grating wave guides or weakly modulated photonic crystals in which anomalous beam propagation was observed. We plot an EFS of a 2D photonic crystal with a finite but small periodic modulation effect in Fig. 4(b). Comparing Fig. 4(b) to Fig. 4(a), one can observe small gaps that appear

near the intersecting points although the overall structure is much the same. The effect of gap opening is that some of the diffracted waves are not excited due to this gap. In other words, we can selectively pick up or exclude some of diffracted waves. This mechanism can be applied to exclude a transmitted wave and excite a diffracted wave only, as illustrated in Fig. 4(c). Figure 4(b) shows that, a k -conservation line is passing through a small gap formed around the K point and it intersects with a circle (dotted) centered at the origin. This circle represents a $G=0$ plane wave corresponding to a transmitted wave. In this small gap region, a transmitted wave [e.g., wave A in Fig. 4(a)] becomes evanescent, and thus only a diffracted wave is excited. Normally, the propagation direction of a transmitted wave does not differ greatly from that of conventional refraction in a dielectric material, and the propagation direction of a diffracted wave can be very different from that of conventional refraction. So, excluding the transmitted wave, the situation itself may seem as if the light beam is being *refracted* in a very strange way. However, this is not a correct view. Such a situation can only be realized at certain incident angles when the transmitted wave falls into a gap. Otherwise, conventional refraction or diffraction should occur. This is obvious from the EFS shape in Fig. 4(b) that is almost the same as the EFS without gaps shown in Fig. 4(a) except the vicinity of the intersecting points. Therefore, we still cannot define a refractive index for such a situation. This discussion of the gap opening also applies for a 1D grating.

To summarize the preceding discussion, what we have shown is that light propagation in weakly modulated photonic crystals is quite similar to that in 1D grating. The beam decomposition and large beam steering observed are due to the band folding and singularities at the intersecting points in k space. The anomalous light propagation reported for photonic crystals, for example the superprism effect, is easy to understand within this picture. Therefore, the light propagation in such photonic crystals cannot be analyzed in terms of the phase refractive index, in the way that conventional refraction in a dielectric can.

V. LIGHT PROPAGATION IN STRONGLY MODULATED PHOTONIC CRYSTALS

What then happens when the periodic modulation becomes large? We know that propagation is still governed by EFS and k conservation across the interface, but the situation is now qualitatively different from the weakly modulated one. Although the gaps influence occurs only near the singular point in the former case, the gap opening now comes to dominate the overall EFS shape. This breaks up the gratinglike picture in Sec. IV, which we will show in this section.

Bloch modes in photonic crystals are expressed as a mixture of transmitted plane wave and diffracted waves having a reciprocal vectors G :

$$\psi_k = \sum_G c_G \exp[i(k+G)r]. \quad (3)$$

In the preceding sections, we assumed that we can characterize excited waves as transmitted waves or as diffracted waves with a certain G . That is, we categorized Bloch waves in terms of their dominant G component since the degree of

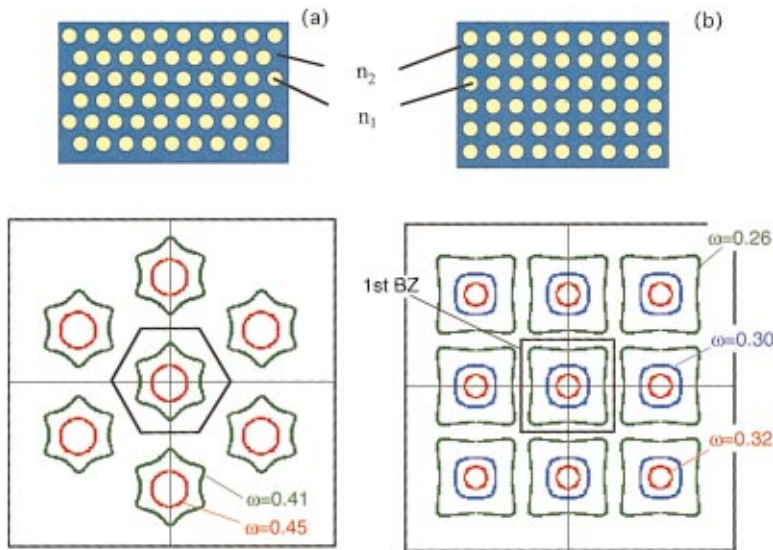


FIG. 5. (Color) Hexagonal (a) and square (b) 2D GaAs air-hole photonic crystals (with a hole diameter of $0.7a$,) and the resulting EFS's at several frequencies. Frequency is normalized as $\omega a/2\pi c$. $\omega_{\text{gap}} \cong 0.48$ for (a) and $\omega_{\text{gap}} \cong 0.34$ for (b) where ω_{gap} is a gap edge frequency.

mixing is not strong. However, excited waves in strongly modulated photonic crystals should be a strong mixture of many diffracted wave components with different G . In such cases, the light propagation angle does not follow the formula for a grating diffraction [Eq. (2)]. In general, EFS cannot be decomposed into a simple ensemble of circles, which excludes a simple gratinglike description or refractionlike description. Seemingly in such cases, the situation can only be characterized as chaotic, and a simple qualitative behavior cannot be extracted.

To examine this, we plot EFS of 2D hexagonal and square GaAs air-hole photonic crystals (with a hole diameter of $0.7a$) at several frequencies near one of the band gaps in Fig. 5. In both cases, the EFS shape becomes rounded as the frequency approaches to the band gap. This is a rather general effect for periodic modulation. The Fermi surface (EFS of the electronic band structure for a solid) of metal exhibits a similar starlike shape reflecting the symmetry of the crystal, which is sometimes referred to as a “monster.” As is well known in solid-state physics, the crystal effect always

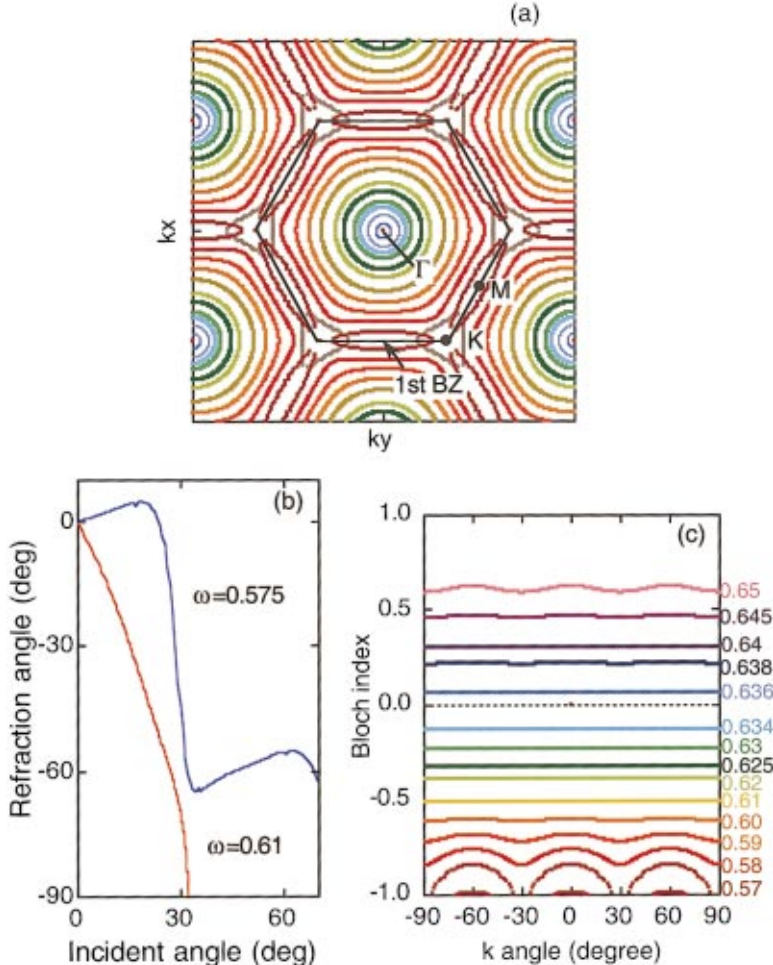


FIG. 6. (Color) (a) EFS plot of TE modes in a 2D GaAs pillar hexagonal photonic crystal ($n_1 = 3.6$, $n_2 = 1$, $r = 0.7a$) at $\omega = 0.56 - 0.635$ (from outer to inner). The colors represent frequency indicated in (c). The first BZ of a hexagonal lattice and the symmetry points are also shown. (b) Refraction angle versus incident angle at $\omega = 0.575$ and 0.61 . (c) Effective refractive index as a function of the angle of the k vector at various frequencies.

round out the monster's sharp corners.²⁰ This can be explained by the fact that the mixing among different G components becomes more pronounced near the bandgap energy around symmetry points in the reciprocal space, which eventually pushes out the sharp corners. This tells that when the periodic modulation effect is not large, the EFS exhibits generally a starlike shape consisting of arcs belonging to diffracted waves; but when it becomes strong, the EFS shape becomes circular or spherical near the gap.²¹

We will now investigate this effect in more detail by examining TE modes of a 2D hexagonal GaAs pillar photonic crystal (with a pillar diameter of $0.7a$) in air. Figure 6(a) shows the EFS for this 2D photonic crystal at $\omega = 0.56-0.635$. As ω approaches 0.635 that corresponds to one of the gap frequencies $\omega(\Gamma_3)$, the shape of EFS becomes rounded and finally becomes circular. In the case of Fig. 6(a), the gap width around $\omega(\Gamma_3)$ is very small, but this does not mean the periodic modulation effect is small. In fact, the modulation effect is significantly large as seen in the figure. This means that the gap width itself is generally not directly related to the strength of the periodic modulation effect but the periodic modulation effect (monster rounding) is most pronounced near the gap frequency (including a gap with very small gap width: In such a case, it might be better referred as symmetry point frequency). We will later examine the strength of the monster rounding for various photonic crystals having different gap width.

From the shape of EFS, we can deduce the propagation angle using the relation $\mathbf{v}_g = \text{grad}_k \omega$. We calculated the relation between the incident and propagation angles for $\omega = 0.61$ and $\omega = 0.575$ as shown in Fig. 6(b). Though the propagation angle at $\omega = 0.575$ is complicated as a result of the complicated shape of EFS, the curve is very simple at $\omega = 0.61$. At $\omega = 0.61$, the EFS consists of a single circle. Note that the EFS plot looks similar to that of a conventional dielectric material as shown in Fig. 3(a). The excited wave is determined by the circular EFS within the first Brillouin zone, and the propagation angle thus should follow Snell's law. This means that we can define an effective refractive index n_{eff} from the radius of the EFS using Snell's law. In Fig. 6(b), we confirmed that the curve for $\omega = 0.61$ follows Snell's law using $n_{\text{eff}} = -0.50$. This curve shows that the propagation angle follows Snell's law at $\theta_{\text{in}} < \arcsin(|n_{\text{eff}}/n_0|)$, and no waves are excited in the photonic crystal at $\theta_{\text{in}} > \arcsin(|n_{\text{eff}}/n_0|)$, which corresponds to total internal reflection for a dielectric material. Note that total internal reflection does not occur when a light beam is incident from air to a conventional material. In this way, the light propagation in this case is properly described by the effective index derived by using Snell's law, suggesting that the beam propagation is refractionlike.

We check the applicable range of this effective index. Figure 6(c) shows the deduced effective index as a function of the in-plane angle of k at various values of ω . This graph indicates that the deduced index does not depend on the k angle in the range $0.59 < \omega < 0.645$. This means that the deduced index is well defined over this range. This range corresponds to 140 nm at $1.55 \mu\text{m}$ (the typical wavelength for optical communication), which is wide enough for considering real applications.

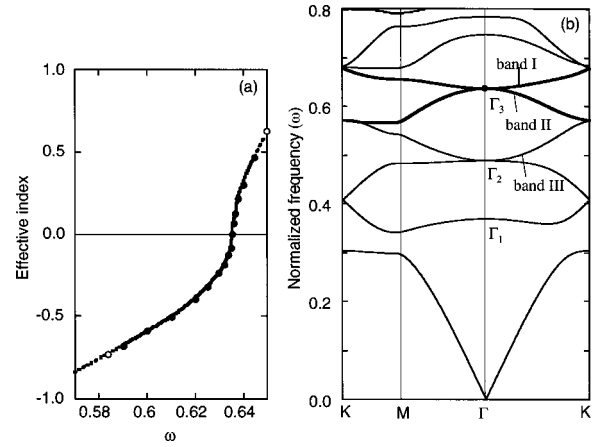


FIG. 7. (a) Effective index versus frequency of TE modes of a 2D GaAs pillar hexagonal photonic crystal ($n_1 = 3.6$, $n_2 = 1$, $2r = 0.7a$). The frequency range where the index becomes non-well-defined is indicated by the broken line. (b) Photonic band structure of the same photonic crystal.

Although we have pointed out similarity to conventional refraction, there is a striking difference from conventional refraction, which we have not pointed out in the preceding paragraph. Note that as ω increases up to $\omega = 0.635$ the radius of the monster shrinks. Considering $\mathbf{v}_g = \text{grad}_k \omega$, this means that propagation direction is inward for this monster, though it is always outward for a conventional dielectric. This results in a negative propagation angle for all incident angles as already shown in Fig. 6(b), which leads to a negative effective index. This unusual negative refraction is a direct consequence that the gap opening dominates the overall EFS structure. In contrast to Fig. 4(b) where the EFS can be approximated by the EFS of an empty lattice, we observe that this EFS in Fig. 6(a) cannot be traced back to the EFS circles of an empty lattice. That is, a conventional transmitted wave does not exist at any angle, and the excited Bloch wave cannot be approximated by any single diffracted wave having specific G , but is a strong mixture of diffracted waves.

Figure 7(a) is a plot of effective index against ω . In the range where the index is well defined, the effective index varies from -0.7 to 0.5 . We compare this ω dependence to the photonic band diagram for this structure as shown in Fig. 7(b). Notice that the sign of the effective index is reversed at $\omega = 0.635$ which corresponds to the $\omega(\Gamma_3)$ point in the band structure. Band I [$\omega > \omega(\Gamma_3)$] has a positive index and band II [$\omega < \omega(\Gamma_3)$] has a negative index. The same characteristics are found for bands near $\omega(\Gamma_2)$. Although the positive and negative index bands are almost touching in both of these cases, touching is not essential. We have confirmed that the effective index becomes well defined in the vicinity of open gaps as well. This is trivial because the monster rounding generally occurs in the vicinity of gaps around symmetry points as mentioned earlier. We show another example that is TM (electric field lies perpendicular to the 2D plane) photonic band diagram of a 2D GaAs air-hole photonic crystal in Fig. 8(a). In this case, band I (III) and band II (IV) near the open gap between $\omega(\Gamma_1)$ [$\omega(\Gamma_3)$] and $\omega(\Gamma_2)$ [$\omega(\Gamma_4)$] are well-defined positive and negative index states, respectively. Figure 8(b) shows the effective index of bands I and II against ω .

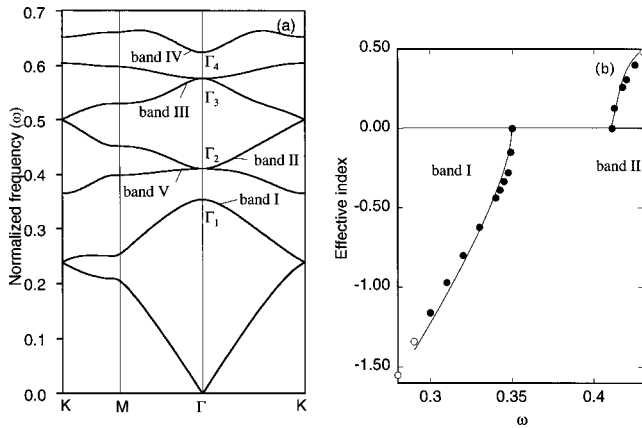


FIG. 8. (a) Photonic band structure of TM modes for a 2D GaAs air-hole hexagonal photonic crystal ($n_2=3.6$, $n_1=1$, $2r=0.8a$). (b) Effective index versus frequency.

It is generally known that an air-hole-type 2D photonic crystal has a larger gap in TE modes, and a pillar type 2D photonic crystal has a larger gap in TM modes. We observe that the formation of well-defined effective index states has the opposite tendency. The air-hole-type crystal prefers TM modes and the pillar type crystal prefers TE modes,²² which is probably because available propagating bands do not exist when the periodic modulation effect is strong for the case optimized for wider gaps due to the efficient gap formation, but such modes still exist for the case optimized for wider effective index region even when the periodic modulation is strong.

Concerning these characteristics, there is an interesting analogy with the electronic band in semiconductors, as shown in Fig. 9. In a semiconductor, a negative effective mass state (the hole band) appears below the energy gap, and a positive effective mass state (the electron band) appears above the gap, which is quite similar to the manifestation of effective index states in photonic crystals. This analogy makes sense if we note that the sign of effective mass in semiconductors and the sign of effective index in photonic crystals are both derived from the band curvature. Furthermore, the effective mass approximation is only valid near the bandgap in the electron band theory. This is similar to our case where the effective index state is only valid near the

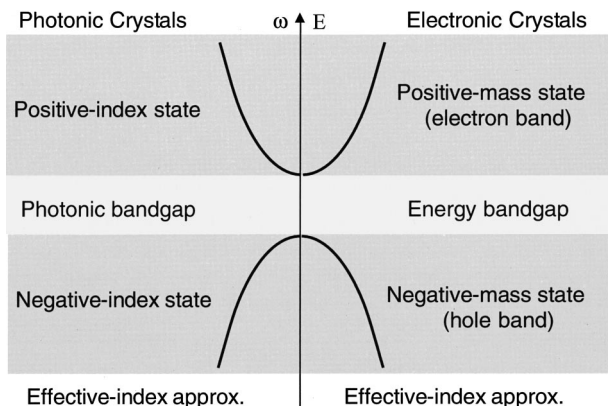


FIG. 9. Analogy between effective mass approximation for Bloch electron bands and effective index approximation for Bloch photon band.

photonic gap. A Bloch electron in a solid is generally very different from a free electron, but it becomes free-electron-like near the bandgap or band minimum and the effective mass approximation can be applied in such regions. In this context, the present situation can be understood that a Bloch photon comes to resemble a free photon (that is, a plane wave) having an effective refractive index near the bandgap despite of large scattering by the periodic lattice, that is, the geometrical optic approach can work near the photonic band-gap.

These results indicate that, if there is a substantially strong periodic modulation in a photonic crystal, it behaves as a continuous isotropic material having an effective refractive index at a certain frequency range near the band edge. In such cases, exotic light propagation phenomena inside the photonic crystal can be simply described by Snell's law using an effective refractive index. In contrast to the weakly modulated case where the definition of refractive index is not meaningful, this effective refractive index has a clear correspondence to the true phase refractive index as far as the index defined in Snell's law is concerned. The sign and absolute value of the effective index can be artificially varied by frequency, crystal structure, and refractive indices of composing materials; it is not limited by the range of the indices of the materials themselves. The effective index can be negative or less than unity. The fundamental limit on this effective index is $|n_{\text{eff}}| \leq \max(n_1, n_2)$. Note that this effective index is not limited by the Hahin-Shtrikman bounds²³ which only holds in the effective medium regime, corresponding to photonic crystals in the long-wavelength limit.

Although the monster rounding generally occurs in the vicinity of any gaps, the strength of this rounding differs from band to band. Some of the bands retain anisotropy rather close to the band edge. For example, the lower band of the Γ_2 point (band V) in Fig. 8(a) forms a surprisingly accurate hexagon in the vicinity of the bandgap. In such cases, a normal effective index cannot be defined but light propagation phenomenon is interesting in itself. Due to its hexagonal shape, the beam propagation direction is frozen at either 0° or 60° over a wide incident angle range. In other words, such a photonic crystal becomes a network of straight wave guides oriented towards its symmetry axes, and propagation in other directions is prohibited by a partial photonic gap.²⁴ Such freezing of the propagation direction cannot be explained by the model for weakly modulated photonic crystals which we used in Sec. IV, where the EFS can be approximated as a sum of circles. It only occurs for strongly modulated photonic crystals where EFS is a strong mixture of many diffracted waves. This anisotropy of the effective index near the gap seems to resemble the anisotropy of effective mass in semiconductors. In semiconductors, this anisotropy originates in the anisotropy of the atomic orbitals which compose a particular electron band (such as s , p , or d orbital). In the usual photonic crystal case, however, such an atomic-orbital-like character²⁵ does not significantly influence the photonic band because of the weak confinement in the lattice point (*photonic atom*). Thus, the anisotropy is mainly due to the character of the band itself determined by the crystal symmetry at least when the wavelength is comparable to the lattice constant, which could be analyzed by the group theoretical approach.²⁶

Although the main concern of this paper is phase index, here we would like to comment on the group refractive index for these photonic crystals. In order to examine it, we have to investigate the frequency dispersion of photonic crystals. Apparently seen from the band diagram, the photonic crystals we are discussing have a strong frequency dispersion, which significantly influences the group velocity index. Although the complicated band curvature is indicating a complicated group velocity, it can be reduced to a considerably simple relation in the vicinity of the bandgap. This is easily understood if one compares again the present situation with that of electron bands in a solid, in which the band should have a parabolic dispersion near the band edge. This parabolic dispersion does not result from the parabolic dispersion of free electrons $E = \hbar^2 k^2 / 2m$, but is attributed to the fact that the periodic modulation induces the energy gap in the second-order perturbation. In the case of photonic crystals, this can be approximately expressed as follows:

$$\omega^2 - \omega_0^2 \approx \eta k^2 \quad (4)$$

(ω_0 is the band edge frequency, and η is an expansion coefficient), which can be reduced to

$$\omega \approx \omega_0 + \frac{\eta}{2\omega_0} k^2 = \omega_0 + \frac{c}{v} k^2. \quad (5)$$

This shows that Bloch photons have an electronlike parabolic dispersion near the band edge. $v (= 2\omega_0 c / \eta)$ contains all information on the band near the gap within this context, and could be seen as an effective *mass* of Bloch photons because it represents a parabolic (rather than a linear) dispersion of bands. This leads to the following dispersion relation of group index n_g :

$$n_g = v / 2k. \quad (6)$$

A expression for the phase index dispersion is not simple, but if we use a scaled frequency $\omega' = \omega - \omega_0$ in analogy to the electron band case, we will get the following another phase index dispersion:

$$n_p' = ck / \omega' = v / k = n_g / 2, \quad (7)$$

which is simply related to the group index n_g by a factor of 2 (due to the parabolicity). This new expression of phase index is mostly useless in the present situation, but it could be meaningful when we discuss the light propagation between different photonic crystals sharing a similar crystal structure in common. Some of readers might notice that there is some similarity to the nonparabolicity problem in the semiconductor heterostructures consisting of materials with different effective mass.²⁷

To see how this parabolic representation is relevant, we replot Fig. 7(b) as ω versus k^2 in Fig. 10. This shows that bands near the band edges are very close to parabolic, and the expressions (5) and (6) are relevant under such a regime. A detailed discussion of frequency dispersion is beyond the scope of this paper, but this already shows that although Bloch photons propagate like free photons at fixed frequency, as far as frequency dispersion is concerned they exhibit a unique parabolic dispersion which is quite different from that of free photons.

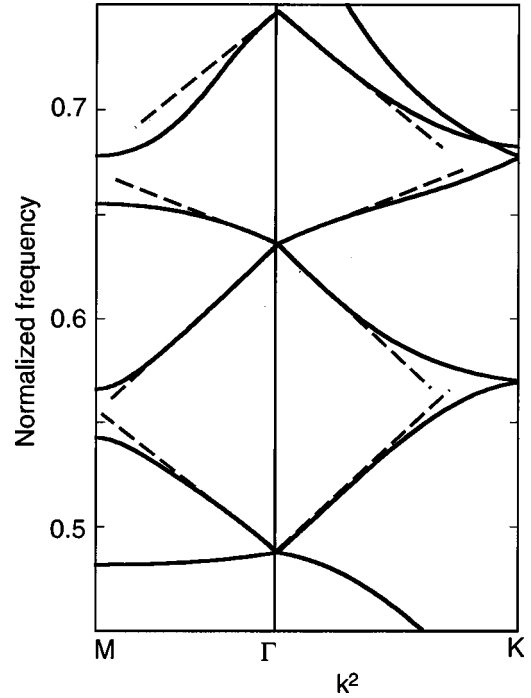


FIG. 10. Replotted version of the band diagram shown in Fig. 7 (b) as a function of k^2 . Straight lines are guide to the eye for indicating the parabolic character of bands near the singular points.

In this section we have shown that, the monster rounding generally occurs near the bandgap, and the effective index becomes well defined in such regions, and the sign of the indices differs between the upper and lower bands. Before moving on to a next section, we would like to point out that this discussion can naturally be extended to 3D photonic crystals and it is thus basically possible to control the 3D propagation of light. However, realization of such states in 3D photonic crystals are more limited than in 2D photonic crystals, since it requires the existence of full photonic bandgaps that are known to be more difficult to obtain in 3D structures.²⁸

VI. NEGATIVE REFRACTION

The fact that we can realize an arbitrary refractive index state leads to many possibilities for the control of light propagation. The most interesting point is that this realizes negative refraction, as illustrated in Fig. 11(a). This negative refraction leads to many anomalous light propagation phenomena. We show some examples: an imaging effect [Fig. 11(b)] and an open cavity formation [Fig. 11(c)]. In the latter

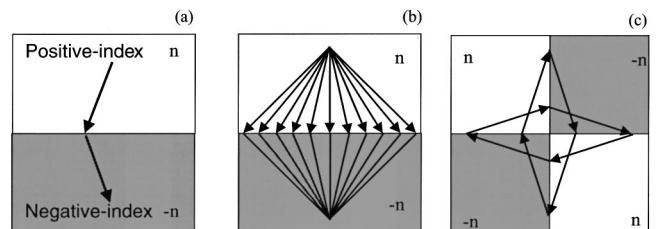


FIG. 11. Schematic diagrams of light propagation in negatively refractive photonic crystals: (a) negative refraction, (b) mirror-inverted imaging effect, and (c) formation of an open cavity.

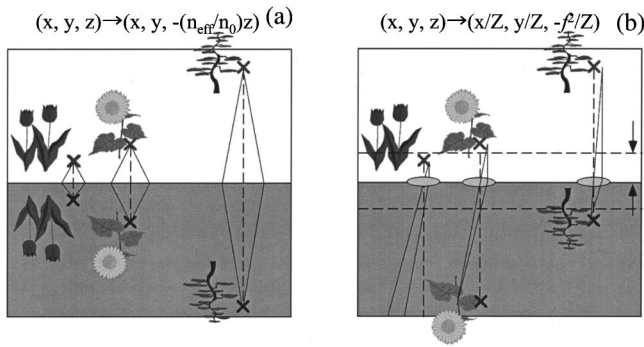


FIG. 12. Schematics of imaging by a negatively-refractive photonic crystal and imaging by a lens.

case, there exist many closed optical paths running across the four interfaces which form a kind of an open cavity despite the fact that there is no reflecting wall surrounding the cavity. In the former case, light is emitted from a point source to a negatively refractive photonic crystal. Within the conventional paraxial-ray treatment, the refracted wave converges at another point in the photonic crystal. This means that objects in the left-hand space produce real images in the right-hand space. This imaging is fundamentally different from conventional imaging by a lens. Figure 12 schematically illustrates two types of imaging. Imaging by a lens is described by Newton's formula, in which the focal length is an important parameter. Magnification depends on the relative distance of an object from the lens and focus point. Therefore it only produces a 2D image on the focal plane and does not produce a 3D image. On the contrary, a negatively refractive photonic crystal produces a 3D image (if it is a 3D negatively refractive photonic crystal) by the mirror-inversion transformation $(x, y, z) \rightarrow (x, y, -\beta z)$ where $\beta = \text{abs}(n_{\text{eff}}/n_0)$, which is different from Newton's formula. In addition, the lens imaging has a definite principal axis, but the present imaging has translational symmetry in the boundary plane. In this sense, this imaging is rather close to imaging by a mirror. The apparent difference between a photonic crystal and a mirror is that the former produces a real image but the latter only produces a virtual image. This unique property is suggesting possibilities of 3D photographing by use of negatively refractive photonic crystals.

We again point out the difference between this negative refraction and the situation for a weakly modulated photonic crystal shown in Fig. 4(c). Although the propagation angle can become negative at a certain incident angle in a weakly modulated photonic crystal, this does not lead to real imaging because negative refraction only occurs over a limited incident angle range and even within this region light rays emitted from the same point but traveling in the different orientation do not converge to the same point.

In the bulk of this paper, we have discussed the light propagation using EFS plots; in other words we examined the wavevector conservation across the interface. This treatment is adequate for determining the propagation angle, but it is not still clear to what extent such Bloch waves will be excited by a plane wave incidence since we have not quantitatively discussed the amplitude continuity across the interface. In principle, this can be done by a proper handling of the amplitude connection between the allowed Bloch waves in the photonic crystal and the outside plane waves considering the effect of the periodic boundary condition in the interface plane. This treatment was the same as that has been established in electron diffraction theory.^{29,30} Instead of doing this, we have numerically simulated electromagnetic wave propagation (in TE mode) in a hexagonal GaAs photonic crystal by a 2D finite-difference time-domain method³¹ using a real refractive index distribution profile of the periodic structures. We used a perfectly matched-layer absorbing condition for the outer boundaries.³² Figure 13(a) shows negative refraction where an angled Gaussian beam is incident to the interface. The negative propagation angle extracted from this result coincides with that is obtained from the EFS calculated by the plane wave expansion. Figure 13(b) shows mirror-inverted imaging. A point source is located in the conventional material, and focusing is clearly observed in the negative-index photonic crystal. These numerical calculations directly solved Maxwell equations including appropriate amplitude continuity without any simplification, and thus these results clearly demonstrate the experimental observability of the phenomena discussed in this paper.

VII. SUMMARY

We have systematically analyzed the light propagation phenomena in periodic structures and photonic crystals with

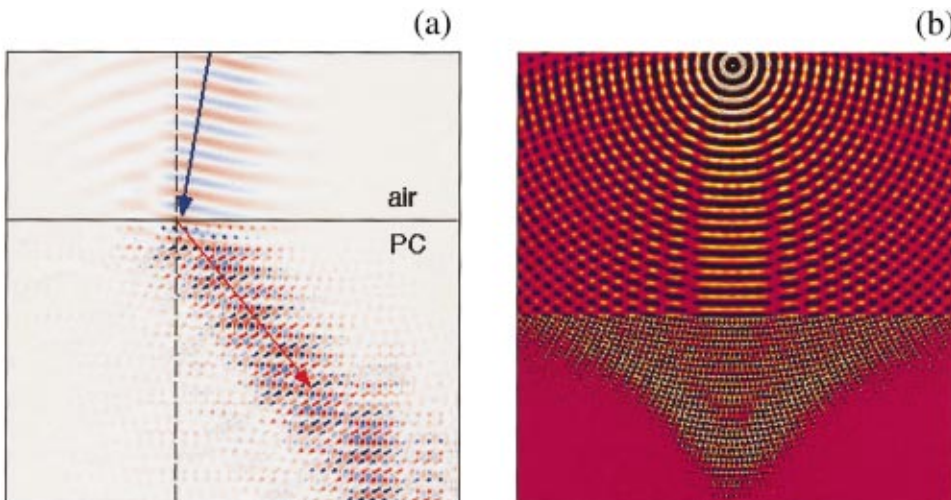


FIG. 13. (Color) Numerical simulation of electromagnetic wave propagation in negatively refractive photonic crystals. Magnetic field (H_z) distribution of TE mode after 2×10^4 steps of calculation. The lower half is a hexagonal photonic crystal with 100×57 unit cells. (a) A slightly tilted Gaussian beam is launched from air ($n_0=1$). (b) A point source emitting at $\omega=0.62$ is located in continuous material with $n_0=0.5$. [If we replace it with air ($n=1.0$), the lower half result will merely be compressed vertically.]

the help of the band theory and numerical simulations. Our motivation is to examine whether light propagation in photonic crystals can be understood by simple geometrical optic analogies. First, we have examined the effect of the band folding that is directly related to the periodic boundary condition of the structure. It has been shown that the propagation characteristics of diffraction gratings and weakly modulated photonic crystals are much alike and can be explained within a similar framework. This explains anomalous propagation phenomena in grating waveguides and photonic crystals. These studies have clarified that the light propagation in these media is fundamentally different from conventional refraction, and therefore we cannot define appropriate refractive index.

However, subsequent studies showed that the light propagation in strongly modulated photonic crystals near the photonic bandgaps, in which the second effect—the gap opening—dominates EFS shape, comes to resemble refraction phenomenon in a dielectric material even in the presence of strong multiple diffraction. In these cases, we can define effective phase refractive index to explain the propagation inside the photonic crystal using the conventional Snell's

law. Since such effective index is determined by the photonic band structure, it can be negative or less than unity, which leads to unusual refraction phenomena including negative refraction. The basic mechanism is similar to the effective mass model in electron band theory. A Bloch photon becomes free-photon-like in the vicinity of the bandgaps, and can be considered to be refracting with an effective refractive index. Such effective index states only exist near the photonic bandgap, in a similar way to the effective mass states in a semiconductor. We have shown that negative index states lead to interesting propagation phenomena, such as imaging effect, which have been confirmed by numerical simulation of electromagnetic wave propagation. These unique properties of refracting Bloch photons have the potential to drastically change the form of optical components.

ACKNOWLEDGMENTS

The author would like to acknowledge T. Nakahara, H. Taniyama, W. Lui, T. Yamanaka, Y. Yoshikuni, H. Kosaka, and S. Kawakami for helpful discussions, and T. Tamamura for his encouragement throughout this work.

*Email: notomi@will.brl.ntt.co.jp; Fax: +81-46-240-4305

¹E. Yablonovitch, *Phys. Rev. Lett.* **58**, 2059 (1987).

²*Photonic Band Gaps and Localization*, edited by C. M. Soukoulis NATO Advanced Studies Institute, Series B: Physics, Vol. 308 (Plenum, New York, 1993).

³J. D. Joannopoulos, P. Villeneuve, and S. Fan, *Nature (London)* **386**, 143 (1997).

⁴K. Ohtaka, *Phys. Rev. B* **19**, 5057 (1979).

⁵P. St. J. Russel, *Phys. Rev. B* **33**, 3232 (1984); P. St. J. Russell, T. A. Birks, and F. D. Lloyd-Lucas, *Confined Electrons and Phonons*, edited by E. Burstein and C. Weisbuch, NATO Advanced Studies Institute Series B: Physics, Vol. 340 (Plenum, New York, 1995).

⁶S.-Y. Lin, V. M. Hietala, L. Wang, and E. D. Jones, *Opt. Lett.* **21**, 1771 (1996).

⁷H. Kosaka, T. Kawashima, A. Tomita, M. Notomi, T. Tamamura, T. Sato, and S. Kawakami, *Phys. Rev. B* **58**, R10 096 (1998).

⁸J. P. Dowling and C. M. Bowden, *J. Mod. Opt.* **41**, 345 (1994).

⁹S. Enoch, G. Tayeb, and D. Maystre, *Opt. Commun.* **161**, 171 (1999).

¹⁰K. Ohtaka, T. Ueta, and Y. Tanabe, *J. Phys. Soc. Jpn.* **65**, 3068 (1996).

¹¹For example, in the result of Ref. 7, the observed light was always propagating in the opposite direction from the band calculation. And many of the theoretically expected waves are not observed in real experiments.

¹²S. Kawakami, *Electron. Lett.* **33**, 1260 (1997).

¹³M. Notomi, T. Tamamura, Y. Ohtera, O. Hanaizumi, and S. Kawakami, *Phys. Rev. B* **61**, 7165 (2000).

¹⁴P. Halevi, A. A. Krokhin, and J. Arriaga, *Phys. Rev. Lett.* **82**, 719 (1999).

¹⁵N. A. Nicorovici, R. C. McPhedran, and L. C. Botten, *Phys. Rev. Lett.* **75**, 1507 (1993).

¹⁶R. C. McPhedran, N. A. Nicorovici, and L. C. Botten, *J. Electron. Waves Appl.* **11**, 981 (1997).

¹⁷A. Yariv and P. Yeh, *Optical Waves in Crystals* (Wiley, New York, 1984).

¹⁸L. P. Bouckaert, R. Smoluchowski, and E. Wigner, *Phys. Rev.* **50**, 58 (1936).

¹⁹M. Plihal and A. A. Maradudin, *Phys. Rev. B* **44**, 8565 (1991).

²⁰J. M. Ziman, *Principles of the Theory of Solids*, 2nd ed. (Cambridge University Press, 1972).

²¹In Ref. 8 the EFS becomes also spherical, but this does not relate to the monster-rounding effect but to the fact that they used an unreal isotropic photonic band model (which cannot be realized in any possible real crystal structure) for approximating 3D photonic band.

²²This does not mean that the monster rounding does not occur in the opposite case (such as TE modes of an air-hole-type photonic crystal). Note that it actually does occur as shown in Fig. 5.

²³Z. Hashin and S. Shtrikman, *J. Appl. Phys.* **33**, 3125 (1962).

²⁴Similar, almost perfectly hexagonal EFSs also appear in the vicinity of the edge of the range where the effective index approximation works, such as $\omega=0.58$ in Fig. 6(a).

²⁵T. Mukaiyama, K. Takeda, H. Miyazaki, Y. Jimba, and M. Kuwata-Gonokami, *Phys. Rev. Lett.* **82**, 4623 (1999).

²⁶K. Sakoda, *Phys. Rev. B* **52**, 7982 (1995).

²⁷U. Ekenberg, *Phys. Rev. B* **40**, 7714 (1989).

²⁸K. M. Ho, C. T. Chan, and C. M. Soukoulis, *Phys. Rev. Lett.* **65**, 3152 (1990).

²⁹H. Bethe, *Ann. Phys. (Leipzig)* **87**, 55 (1928).

³⁰D. S. Boudreaux and V. Heine, *Surf. Sci.* **8**, 426 (1967); G. Capart, *ibid.* **13**, 361 (1969).

³¹A. Taflove, *Computational Electrodynamics* (Artech House, Boston, 1995).

³²J. P. Berenger, *J. Comput. Phys.* **114**, 185 (1994).